CHAPTER 6

QUANTITATIVE METHODS—
MICROINDENTATION HARDNESS

6.1 INTRODUCTION

The hardness of an ore mineral has been estimated or measured by mineralogists in one of three ways: through examination of (1) polishing hardness, (2) scratch hardness, or (3) microindentation hardness. Polishing hardness, discussed in detail in Chapter 3, only enables the hardness of a phase to be estimated relative to other phases in a polished section. Scratch hardness may also be qualitatively estimated by visual examination of the relative intensity of surface scratches on a polished section (see Chapter 3). The *Mohs scale* of scratch hardness, universally employed in the study of minerals in hand specimen, is a simple quantification of this property. Early attempts at measuring mineral hardness under the microscope involved drawing a scribe across the surface while applying a known load, as in the work of Talmage (1925). Such methods have been superseded by the more accurate techniques of microindentation hardness measurement, in which a static indenter is lowered onto the mineral surface under a known load and the size of the resulting impression is determined.

The measurement of hardness on the microscopic scale has involved a variety of instruments and types of indenter, the most common indenters being the Vickers (a square-based pyramid) and the Knoop (an elongated pyramid). Most systematic studies of ore minerals (Bowie and Taylor, 1958; Young and Millman, 1964) have employed Vickers microhardness determination, and this technique has been widely adopted in ore microscopy. It is important to note that, although the various types of hardness (polishing, scratch, microindentation) will produce very similar results for a series of minerals, differences in relative hardness may be observed on detailed ex-

amination, since the methods (and nature of "deformation" involved) are not equivalent.

6.2 VICKERS HARDNESS MEASUREMENT

6.2.1 Theory

The measurement of Vickers hardness provides a Vickers hardness number (VHN) for a material. The hardness number is defined as the ratio of the load applied to the indenter (gram or kilogram force) divided by the contact area of the impression (square millimeters). The Vickers indenter is a square-based diamond pyramid with a 130° included angle between opposite faces, so that a perfect indentation is seen as a square with equal diagonals (although it is actually a pyramidal hole of maximum depth one-seventh the diagonal length).

The area of the Vickers indentation can be expressed in terms of the length of the diagonal d (in µm) as:

$$\frac{1}{2} d^2 \cos ec \; 68°$$ (6.1)

The VHN, being the ratio of load L (in gram force, gf) to area of indentation, is given by

$$VHN = \frac{2 \sin 68° \times L}{d^2} = \frac{1.8544 \times L}{d^2} \; \frac{g}{µ^2}$$

or

$$\frac{1854.4 \times L}{d^2} \; \frac{g}{mm^2} \; (the \; normal \; units \; employed)$$ (6.2)

Microindentation hardness testers normally employ loads of 100–200 gf, which result in indentations of diagonal lengths approximately 5–100 µm, commonly a few tens of microns in diameter. The load employed in a VHN determination must be stated, since, as we will discuss later, values obtained are not independent of load.

A number of workers have compared the scale of VHN values with the more familiar Mohs scale. As shown in Figure 6.1, Young and Millman (1964) suggest that an approximately linear relationship is found when log Mohs is plotted against log VHN, a relationship expressed by the equation

$$\log VHN = 2.5 \log Mohs + 1.00$$ (6.3)
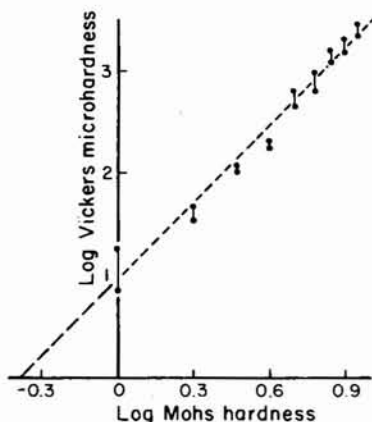
FIGURE 6.1 Correlation of Vickers microhardness with Mohs scale of hardness showing the virtually linear relationship between log Mohs and log VHN. (After Young and Millman, 1964.)

A log/linear relationship was determined by Bowie and Simpson (1977):

$$\log VHN = Mohs \log 1.2 + C \tag{6.4}$$

6.2.2 Instrumental Techniques

A variety of instruments for measuring Vickers hardness are commercially available; some are marketed as complete instruments, and others are designed as attachments to a standard ore microscope. In all instances, a reflected-light microscope forms the basis of the instrument, with a permanent or a detachable indenter head that can be rotated into position in place of a normal objective; the second major addition is a micrometer eyepiece that enables the indentation diagonals to be accurately measured. The load may be applied directly when a plunger is depressed to allow the indenter to descend onto the sample surface, or it may be applied pneumatically via an air line by depressing a lever on an impeller drum.

An example of the typical sequence of operations in a single hardness determination with the Leitz instrument would be as follows:

1. Selection of a suitable grain or area for measurement (of sufficient size and free of cracks or flaws), using a low-power objective (on the surface of a *leveled* polished section)
2. Selection of a high-power ($\times$ 40) objective, focusing, and checking that the area is free from flaws
3. Rotation of indenter nosepiece into position

4. Selection of a suitable load (commonly 100 g, although a range of loads from 10 to 200 g is available for softer or harder materials)
5. Pressing of cable release (or equivalent) to initiate indenting process, after a set time (say, 15 sec) pressing again to withdraw the indenter
6. Examination of indentation under high-power objective
7. Measurement of the length of each diagonal using the micrometer eyepiece, when the indentation has been suitably positioned

The data on diagonal lengths (averaged for each indentation) can be used in Equation 6.2 to calculate the VHN, although tables are normally provided by manufacturers for direct conversion of diagonal measurements to VHN values. An experienced operator can obtain satisfactory results from a couple of indentations on each of three or four grains, except when a wide range of hardness is exhibited by the material.

VHN values have been obtained for most ore minerals, and the accepted standard values have been published by the Commission on Ore Mineralogy (COM) in the IMA/COM Data File (see Section 5.3, Figure 5.9, and Criddle and Stanley, 1993). In Appendix 1 of this book, VHN values are provided for the more common ore minerals, and in Appendix 2 these minerals are listed in order of increasing VHN.

6.2.3   Sources of Error and Accuracy, and Precision of Measurement

Assuming that the instrument is working correctly and has been properly calibrated (a standard block of known VHN is normally provided to check this), errors may still arise from a number of sources, including vibration effects, inconsistent indentation times, and misuse of the micrometer eyepiece. Vibration may be a serious source of error, and the system is best mounted on a bench designed to minimize this effect. Indentation time is important, because a certain amount of creep occurs during indentation and there may be some recovery after indentation. A loading time of 15 sec has been approved by the COM. Errors arising in the actual measurement of the indentation depend partly on factors outside the control of the operator, such as the resolving power of the objective and the quality of the indentation (which may always be poor in certain materials). However, accurate focusing and careful location of the ends of the diagonals are important for acceptable results. Precise measurement can also be improved by using monochromatic illumination (Bowie and Simpson, 1977, suggest using light of $\lambda = 500$ nm and a dry objective of NA $= 0.85$ for relatively rapid and precise results).

Producing an average hardness number for a particular mineral is easier than establishing a true range of hardness, and reproducing the same average values (to within 5%) on the same instrument is fairly simple. Bowie and Simpson (1977) have noted that, if $H_1, H_2, H_3, \ldots H_n$ are the values obtained in n tests on the same specimen and the respective differences from the mean

$(\bar{H})$ are $(H_1 - (\bar{H}), (H_2 - \bar{H}) \ldots (H_n - \bar{H})$, then the standard error of any individual observation is

$$\frac{\sum(H - \bar{H})^2}{n} \tag{6.5}$$

and the standard error of the mean is:

$$\frac{\sum(H - \bar{H})^2}{n^2} \tag{6.6}$$

Relatively large variations may result by using different types of indenter and as a result of applying different loads, as discussed in the next section. Generally, a load of 100 gf should be employed unless the specimen is too soft, too brittle, or too small for this to be acceptable.

6.3 SHAPES OF HARDNESS MICROINDENTATIONS

A perfectly square, clear indentation very rarely results from hardness testing of minerals; the shape of the impression and any fracturing characteristics that may result from indentation can provide useful additional information regarding the identity (and sometimes orientation) of minerals. Young and Millman (1964) have examined the shape and fracture characteristics of indentations in a large number of ore minerals. These authors have noted that the shape characteristics consist of combinations of four distinct indentation types: (1) straight edge, (2) concave edge, (3) convex edge, and (4) sigmoidal edge (see Figure 6.2). The extent to which curvature is developed in these indentations without straight edges can also be classified as weak or strong.
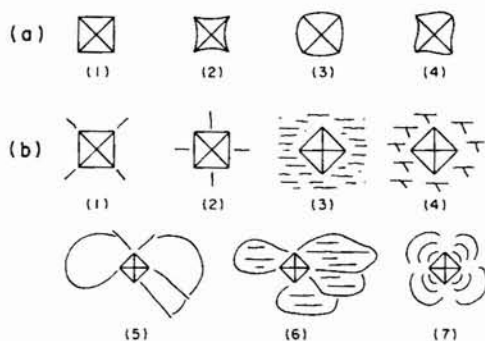
FIGURE 6.2 (a) Indention shape characteristics: (1) straight, (2) concave, (3) convex, (4) sigmoidal. (b) Indentation fracture characteristics: (1) star radial, (2) side radial, (3) cleavage, (4) parting, (5) simple shell, (6) cleavage shell, (7) concentric shell. (Based on Young and Millman, 1964.)

TABLE 6.1   Categories of Indentation Shape, Fracture Characteristics, and Anisotropy Associated with Mineral Structural Groups[a]

Mineral Structural Group	Indentation Anisotropy	Characteristics of Indentation				Characteristics of Fractures
		Straight	Concave	Convex	Sigmoidal	
Metals and semimetals	Mod. to st.	—	Wk. to st.	Wk. to st.	Wk. to st.	Wk. GPT
Simple sulfides	Wk. to st.	—	Wk. to st.	Wk. to st.	Wk. to st.	Wk. rad. and GPT
Co-Ni-Fe sulfides						
Pyrite-type	Iso.	Com.	Wk.	—	—	St. rad. shells
Spinel-type	Iso.	Com.	Wk.	—	—	St. rad. shells
Marcasite-type	Mod. to st.	Com.	Wk.	Wk.	—	St. rad. shells
Complex sulfides						
Sphalerite-type	Wk. or iso.	—	Wk. to st.	—	—	Com. rad. and shells
Wurtzite-type	Mod. to st.	Com.	St.	Wk.	—	St. rad. shells
Niccolite-type	Mod. to st.	—	St.	Wk.	Wk.	Com. rad. and GPT
Sulfosalts						
Chain-type	Mod. to st.	Com.	Wk. to st.	Wk. to st.	—	Com. rad. and shells
Sphalerite-type	Iso.	Com.	Wk. to st.	Wk. to st.	—	Com. rad. and shells
Spinels, isometric oxides, rutile-type oxides, metamict oxides	Wk. or iso.	Com.	Wk. to st.	—	—	Wk. rad.
Hydrated oxides, hex. hematite and zincite-type oxides	Wk. to st.	—	Wk. to st.	—	—	Occ. rad. shells
Silicates, sulfates, phosphates, carbonates	Wk. or iso.	—	Wk.	—	—	St. rad. shells

[a]Abbreviations: wk., weak; mod., moderate; st., strong; iso., isotropic; com., common; rad., radial fractures; shells, shell fractures; occ., occasional; GPT, glide plane traces.

Fracturing or deformation may also occur during indentation, particularly if the mineral has a distinct cleavage or fracture. Again, Young and Millman (1964) have classified the types observed: (1) star radial fractures, (2) side radial fractures, (3) cleavage fractures, (4) parting fractures, (5) simple shell fractures, (6) cleavage shell fractures, and (7) concentric shell fractures. The various shape, deformation, and fracture characteristics of indentations are illustrated in Figure 6.2, and their development in the major ore mineral groups is shown in Table 6.1. Some data on fracture characteristics are also provided in the tables in Appendix 1.

The shapes and fracture characteristics of minerals may vary with orientation of the grain, particularly in such materials as covellite or molybdenite, which have highly anisotropic structures.

## 6.4   FACTORS AFFECTING MICROINDENTATION HARDNESS VALUES OF MINERALS

6.4.1   Variation with Load

The actual VHN value determined for a mineral is not independent of the load used in measurement; generally, an increase in hardness is shown with a decrease in the applied load. For this reason, measurements are often made at a standard load of 100 gf, although Young and Millman (1964) have pointed out the advantages of using a series of standard loads (15, 25, 50, and 100 gf), depending on the hardness of the mineral under examination. These authors undertook a systematic study of hardness variation with load in a variety of minerals and found, for example, that a mean percentage increase in VHN in going from 100 gf load to 15 gf is ~24% for a mineral in the 600–1,200 kg/mm^2 hardness range and ~12% for a mineral in the 60–120 kg/mm^2 hardness range. They also examined the effects of both load and orientation on the VHN values of galena, as shown in Figure 6.3 and discussed in the following paragraph.

One source of this load dependence of hardness is the deformation of the surface layer of a mineral during polishing. The hard layer (~10–20 μm thick) produced by some polishing methods may become important when small loads are used but should have less influence at loads of 100 gf, as shown by tests using different polishing techniques (Bowie and Taylor, 1958). The load dependence may also be related to the actual mechanism of deformation during indentation or may even originate from instrumental effects (Bowie and Simpson, 1977).

6.4.2   Variation with Mineral Texture

Ideally, relatively large and well-crystallized grains are required for hardness determination. When masses of microcrystalline or cryptocrystalline material are measured, the hardness may be markedly lower (e.g., microcrystalline
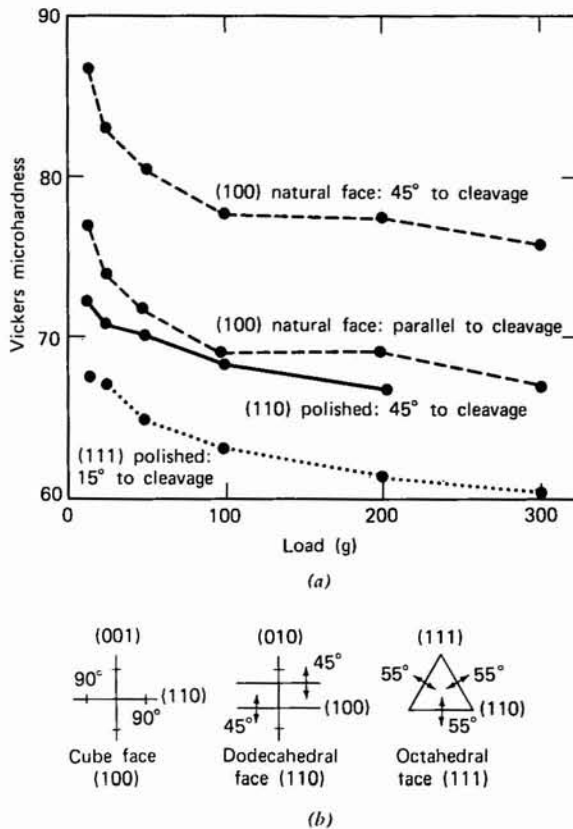
FIGURE 6.3 (*a*) Variation of Vickers microhardness with load and orientation in a crystal of galena. (*b*) Attitudes of (001) cleavage glide planes in galena in sections parallel to cube, dodecahedral, and octahedral planes. (From *Mineral Chemistry of Metal Sulfides* by D. J. Vaughan and J. R. Craig, 1978, Cambridge University Press, after Young and Millman, 1964; used with permission.)

hematite and goethite give VHN values ~70% of values for coarse crystals). On single grains, excessive fracturing normally occurs and values are unreliable if the indentation diagonal exceeds one-third the grain size. In practice, the minimum grain size is ~100 μm, although use of smaller loads may make it possible to obtain results on smaller grains.

6.4.3 Variation with Mineral Orientation

Most minerals show some degree of hardness anisotropy, and this effect may be considerable in fibrous, layered, or prismatic phases [e.g., molybdenite VHN (0001) 33–74, VHN (1010) 4–10 at 100 gf load]. The measurements of Young and Millman (1964) involved determinations on oriented sections of 50 minerals and demonstrated that most minerals give different hardness values

on different crystal faces and different indenter orientations on the same face. Indentation shape and fracture characteristics often also exhibit variations with crystal orientation.

An interesting aspect of hardness anisotropy is that it is not limited to non-isometric minerals; cubic minerals, such as galena, sphalerite, and native copper, show considerable hardness anisotropy. In the case of galena, a detailed interpretation of the variation of hardness with orientation (illustrated in Figure 6.3) has been presented based on the attitudes of various glide planes in the structure. The relationship between hardness values for various faces was determined to be VHN (001) $\gg$ VHN (110) > VHN (111) (see Figure 6.3), and plastic deformation in galena is known to take place by gliding along (100) and (111) planes, the (100) planes being dominant. Hence, on indenting the cube face (001, 100, 010), there is little tendency for movement along (100) planes that are perpendicular or parallel to the surface. On indenting the (110) face, deformation occurs readily by movement along two sets of (100) glide planes oriented at 45° to the indentation direction. On the (111) face, three (100) planes make angles of 35° with the indentation direction and are all capable of easy glide translation, resulting in the lowest hardness of all. The relationships of glide planes to crystal faces are also shown in Figure 6.3.

6.4.4   Variation with Mineral Composition

The variation of hardness with mineral composition has been examined in a number of mineral series and solid solutions. In some cases, hardness variation can be directly linked to variations in structure and bonding in the series. For example, in the series galena (PbS)-clausthalite (PbSe)-altaite (PbTe), which all have the halite-type structure, decreasing VHN (at 100 gf) follows roughly the increasing unit cell parameters (PbS, VHN 57–86, a_o = 5.94Å; PbSe VHN 46–72, a_o = 6.45Å; PbTe VHN 34–38, a_o = 6.45Å). In the series of isostructural disulfides, hauerite (MnS_2)-pyrite (FeS_2)-cattierite (CoS_2)-vaesite (NiS_2) hardness variations can be correlated not only with unit cell parameter but also with the electron occupancy of certain orbitals associated with the metals (see Table 6.2 and Vaughan and Craig, 1978). These variations in the electronic structures of the disulfides also explain differences in metal-sulfur bond strengths, which, like the hardness values, decrease in the sequence FeS_2 > CoS_2 > NiS_2. An intimate relationship clearly exists between hardness, bond strength, and the nature of bonding in minerals, but its precise formulation is complex.

Detailed studies of hardness variation have been undertaken on a number of solid-solution series. As summarized by Vaughan and Craig (1978), several authors have studied the variation of the hardness of sphalerite (Zn,Fe)S with iron content. As illustrated in Figure 6.4a, all of these studies show a sharp increase in hardness on substitution of small amounts of iron (< 2 wt %), and most studies show a subsequent decrease with further iron substitution. The cell parameters of sphalerites show a linear increase with iron substitution (Figure 6.4a), and possibly the initial hardness increase is due to some iron

TABLE 6.2   Vickers Hardness Values for Pyrite-Structure Disulfides and the Correlations Between High VHN, Smaller Unit-Cell Parameter, Metal-Sulfur Distance and Number of Electrons in Antibonding Orbitals, and Higher Cohesive Energies[a]

|	MnS_2	FeS_2	CoS_2	NiS_2
Vickers hardness	485–	1604–	766–	594–
(kg mm^2)	623	2759	1380	1028
Cell size	6.1014	5.4175	5.5345	5.6873
Metal-sulfur distance				
(Å)	2.59	2.262	2.315	2.396
Cohesive energy from thermodynamic data at 25°C, Kcal mol^{-1}	—	246	243	242
Number of electrons in e_g (antibonding) orbitals	2	0	1	2

[a] After Vaughan & Craig (1978).

atoms filling defect sites before the expansion in the unit cell becomes dominant and hardness decreases. Young and Millman (1964) also report the complex hardness variations observed with compositional variation in the hübnerite-wolframite-ferberite $(Fe,Mn)WO_4$ series. Their measurements, illustrated in Figure 6.4b, were performed on oriented crystals.

Clearly, the variation in hardness with composition in solid-solution series is complex and could never be used to give more than a very crude estimate of composition. What may be of greater value is the information on crystal chemical variations implied by such studies.

6.4.5   Variation with Mechanical and Thermal History

The presence of structural imperfections in crystalline materials has a very marked influence on hardness properties. Defects, particularly the linear regions of mismatching of the crystal lattice known as *dislocations* are introduced by mechanical deformation (a process known as *work hardening*). This means that the cutting, grinding, and polishing of specimen preparation can increase hardness values by 5–30%, compared to the values for untreated crystal or cleavage faces of some materials. Since most laboratories use both comparable and consistent methods of specimen preparation, the consequences generally do not seriously impair the use of the technique in mineral identification.

The formation of dislocations, the processes of work hardening, and the effects of both the conditions of initial crystallization and any subsequent heat treatment on defect formation have been extensively studied by metallurgists. In studying natural materials that have undergone mechanical deformation (and sometimes heat treatment) during tectonism and metamorphism, Stanton and Willey (1970, 1971) have demonstrated another important field of
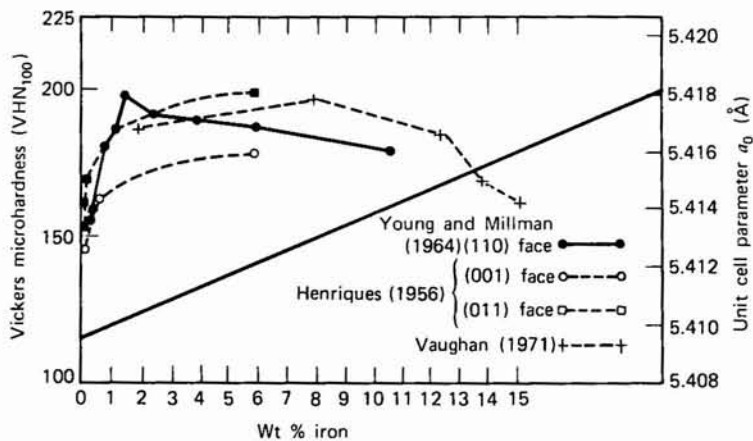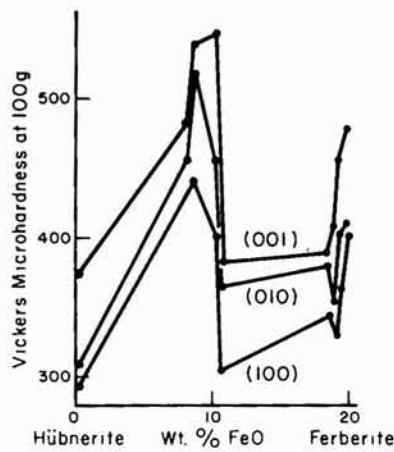
FIGURE 6.4 (a) Variation in Vickers microhardness (at 100 gf load) and cell size (Å) with iron content of sphalerite. (After Vaughan and Craig, 1978) (b) Variation of Vickers microhardness with iron content in the wolframite series (in various orientations). (From *Mineral Chemistry of Metal Sulfides* by D. J. Vaughan and J. R. Craig, copyright © 1978, Cambridge University Press, after B. B. Young and A. P. Millman, 1964; used with permission.)

application of hardness determination of ore minerals. For example, galena deformed by tectonic movement has commonly undergone a process of natural work hardening. This hardening may be eliminated by heat treatment and the softening results from two separate processes—recovery and recrystallization. Although recrystallization initially results in softening, complete recrystallization may ultimately lead to substantial hardening, as Stanton and Willey (1971) have shown in their studies of the recrystallization of naturally deformed sphalerite and galena. In Figure 6.5, the softening-hardening be-
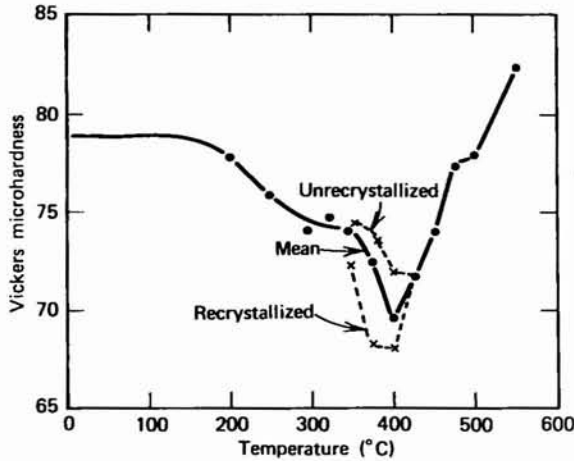
FIGURE 6.5 Softening-hardening behavior accompanying recovery-recrystallization of naturally deformed galena from Broken Hill, Australia. Specimens were heated for one day, and the plotted values are an average of 70 indentations. (From *Mineral Chemistry of Metal Sulfides* by D. J. Vaughan and J. R. Craig, copyright © 1971, Cambridge University Press, after Stanton and Willey, 1971; used with permission.)

havior that accompanies the recovery-recrystallization of naturally deformed galena from Broken Hill (New South Wales, Australia) is illustrated. The curves show the distinct separation in hardness between naturally unrecrystallized and recrystallized material once experimental recrystallization has commenced, and the greater hardness testing of sulfides that have undergone natural deformation or annealing may give valuable information on their postdepositional histories. Information such as the upper temperature limits reached since deformation, whether recovery has occurred, whether a polycrystalline aggregate is a result of primary deposition or recrystallization, and to what extent this recrystallization has proceeded is obtainable from such studies.

In related studies, Kelly and Clark (1975) and Roscoe (1975) have examined the nature of deformation in chalcopyrite; Kelly and Clark (1975) have also summarized data for pyrrhotite, galena, and sphalerite. These workers, although not actually measuring hardness, have carefully examined the strengths of minerals as functions of temperature and confining pressure (see Figure 10.29).

6.5 CONCLUDING REMARKS

The measurement of Vickers hardness provides an established and tested method for quantitative determination of the hardness of minerals in polished section. This has been widely used as an aid to mineral identification

(see Section 5.3), although in many laboratories hardness determination is now used only when optical methods fail to provide conclusive identification.

The applications of microhardness measurement, however, are much more wide-ranging than simply as an identification tool. Hardness exhibits interesting variations when considered in relation to the crystal chemistry of minerals, and the possibilities for further investigations of microhardness in relation to deformation processes and the deformational (and thermal) history of minerals are even more interesting. Studies of ore minerals from deformed rocks have been mentioned already. Another field that has been explored recently by workers in rock and mineral deformation is the use of Vickers microhardness measurement to study deformation mechanisms, particularly in the study of fracture mechanics in rock-forming minerals (Swain and Lawn, 1976; Atkinson and Avdis, 1980; Ferguson, Lloyd, and Knipe, 1987). In such studies, indentation is used to produce deformation in an individual mineral grain under controlled conditions (which have included elevated temperatures). Not only are indentation dimensions and gross characteristics
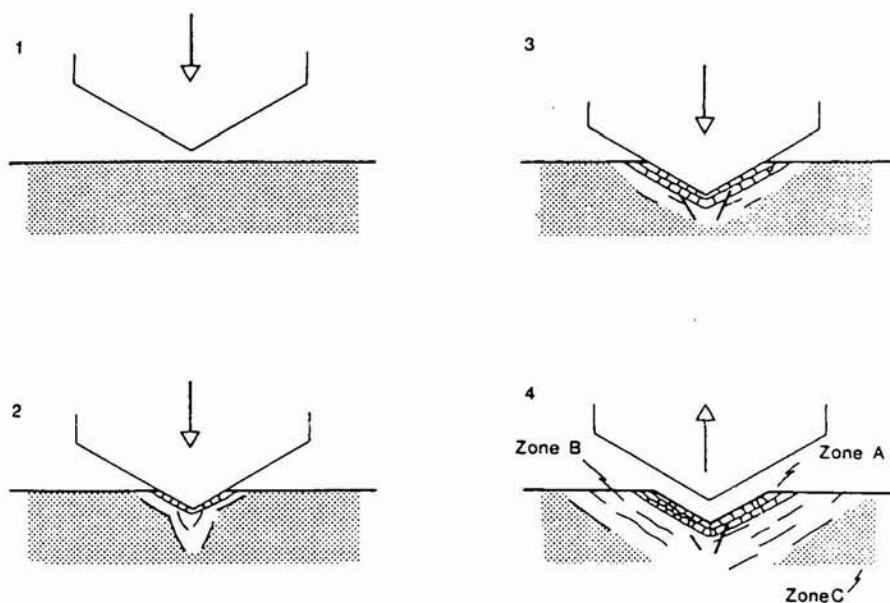
FIGURE 6.6 Schematic illustration of the microstructures evolved in quartz during Vickers indentation. Zone A is characterized by very high fracture density, with some fractures showing evidence of partial melting (microfracturing on a very fine scale apparently is the main mechanism for the plastic deformation associated with indentation). Zone B is characterized by a much lower fracture density; concentric and radial cracks may be, in part, due to unloading and elastic recoil. Zone C has no deformation effects other than large to medium radial fractures that may have nucleated at the specimen surface. (After Ferguson, Lloyd, and Knipe, 1987.)

studied, but also the areas around the indentation are subjected to detailed study using techniques such as scanning and transmission electron microscopy. For example, the studies of quartz by Ferguson, Lloyd, and Knipe (1987) using such techniques has led to an understanding of the microstructure evolved during indentation, as shown schematically in Figure 6.6.

The hardness of a mineral is a complex property of both theoretical and practical interest. Detailed studies of hardness variation with orientation, compositional variation, and thermal and mechanical history of minerals should be a valuable field of future study with wider geological applications than have been exploited so far.

REFERENCES

Atkinson, B. K., and Avdis, V. (1980). Fracture mechanics parameters of some rock-forming minerals determined using an indentation technique. *Internat. J. Rock Mechanics Mining Sci.* **17**, 383–386.

Bowie, S. H. U., and Simpson, P. R. (1977). Microscopy: Reflected Light. In J. Zussman (ed.), *Physical Methods in Determinative Mineralogy*, 2nd ed. Academic, London, pp. 109–165).

Bowie, S. H. U., and Taylor K. (1958). A system of ore mineral identification. *Min. Mag. (Lond.)* **99**, 237.

Criddle, A. J., and Stanley, C. J. (1993). *Quantitative Data File for Ore Minerals*, (3rd ed.) Chapman & Hall, London.

Ferguson, C. C., Lloyd, G. E., and Knipe, R. J. (1987). Fractive mechanics and deformation processes in natural quartz: a combined Vickers indentation, SEM and TEM study. *Canad. J. Earth Sci.* **24**, 544–555.

Kelly, W. C., and Clark, B. R. (1975). Sulfide deformation studies: III experimental deformation of chalcopyrite to 2,000 bars and 500°C. *Econ. Geol.* **70**, 431–453.

Roscoe, W. E. (1975). Experimental deformation of natural chalcopyrite at temperatures up to 300°C over the strain rate range 10^{-2} to 10^{-6} sec^{-1}. *Econ. Geol.* **70**, 454–472.

Stanton, R. L., and Willey, H. G. (1970). Natural work hardening in galena and its experimental reduction. *Econ. Geol.* **65**, 182–194.

———. (1971). Recrystallization softening and hardening in sphalerite and galena. *Econ. Geol.* **66**, 1232–1238.

Swain, M. V., and Lawn, B. R. (1976). Indentation fracture of brittle rocks and glasses. *Internat. J. Rock Mechan. Mining Sci.* **13**, 311–319.

Talmage, S. B. (1925). Quantitative standards for hardness of the ore minerals. *Econ. Geol.* **20**, 535–553.

Vaughan, D. J., and Craig, J. R. (1978). *Mineral Chemistry of Metal Sulfides*. Cambridge University Press, Cambridge, England.

Young, B. B., and Millman, A. P. (1964). Microhardness and deformation characteristics of ore minerals. *Trans. Inst. Min. Metall.* **73**, 437–466.